
Modulated Magnetism in a Nano-structured Butterfly Manganite

Over what distance can we spread charge through delta-doping?

2010 SANS & Reflectometry Summer School • NIST Center for Neutron Research •

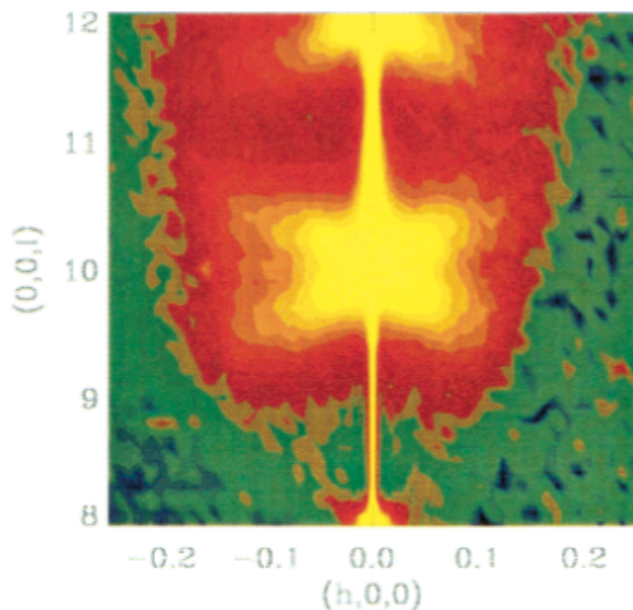


Figure 1: Lepidopteran pattern in diffuse x-ray scattering from lattice distortions in $\text{La}_{1.2}\text{Sr}_{1.8}\text{Mn}_2\text{O}_7$ - hence the term “butterfly manganite”. [1]

Introduction

Fifty years ago, Pierre-Gilles de Gennes recognized that the magnetic properties of manganites could be controlled via the addition or subtraction of mobile carriers.[2] For example, the naturally antiferromagnetic insulator LaMnO_3 can be tuned to be ferromagnetic (i.e., spins aligned parallel from one lattice site to the next) or antiferromagnetic (spins aligned antiparallel from one site to the next) by adding replacement Sr at some fraction of the La sites. For $\text{La}_{1-x}\text{Sr}_x\text{MnO}_3$ (LSMO) the half-doped case constitutes a transition point in the phase diagram, below $x =$

0.5, the compound is ferromagnetic, and antiferromagnetic above.[3] Tuning of the stoichiometry is commonly achieved through spatially random doping of the LaMnO_3 parent compound. Very recently however, Tiffany Santos of Argonne National Laboratory and co-workers have synthesized *digitally ordered* analogs of $\text{La}_{1-x}\text{Sr}_x\text{MnO}_3$ by alternating single unit cell layers of LaMnO_3 (LMO) and SrMnO_3 (SMO), using ozone-assisted molecular beam epitaxy.[4] Here, we consider a digitally-ordered multilayer film on a SrTiO_3 substrate, with $x = 0.47$ (slightly more La than Sr) - a composition that is ferromagnetic for spatially random doped bulk specimens. The La richness (i.e. $x < 0.5$) is achieved by making every 4th LMO layer two unit cells thick instead of one, as shown in Figure 2. In bulk, spatially random addition of La in this region of phase space increases the mobile electron concentration and promotes ferromagnetism. The question is - for

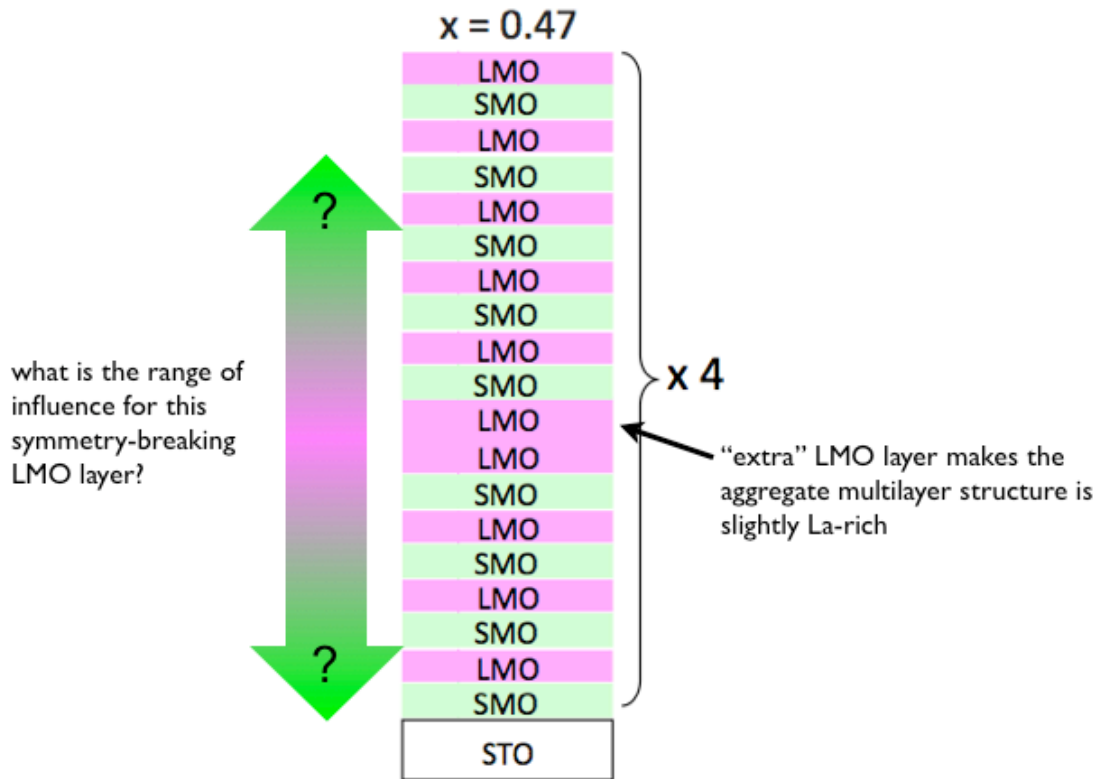


Figure 2: Spatially ordered $\text{La}_{0.53}\text{Sr}_{0.47}\text{MnO}_3$ sample.

an ordered multilayer sample, how does the spatially *coherent* addition of La affect the magnetic properties of neighboring unit cells? Put differently, what is the range of influence of the symmetry breaking extra LMO layer? To answer this question, we will utilize specular polarized neutron reflectometry (PNR), an experimental technique sensitive to the structural and magnetic depth profiles of thin films and multilayers.

Polarized Neutron Reflectometry

For a detailed treatment of neutron reflectometry, see *The Theory of Small Angle Neutron Scattering and Reflectometry* by Andrew Jackson, which has been provided for you, and for *polarized* neutron reflectometry in particular, see the chapter by Fitzsimmons and Majkrzak in *Modern Techniques for Characterizing Magnetic Materials* (available online at <http://www.ncnr.nist.gov/instruments/nglrefl/Fitz.pdf>). In short, reflectometry is sensitive to the depth-dependent index of refraction n , for thin film and multilayer samples. For light of a given wavelength, the index of refraction of a material is a function of that material's electron density. However, for a neutron beam, the index of refraction is dependent on the *nuclear* composition of a material, and (since the neutron has a magnetic moment) on the magnetization of a material. Further, since neutrons have no electrical charge, a neutron beam is highly penetrating, and in most cases, can be used to probe interfaces buried under even microns of material. While useful for fundamental illustration, neutron scatterers do not typically refer to scattering strength in terms of index of refraction. Instead, for reasons of mathematical convenience, the scattering properties of a given isotope are

discussed in terms of a characteristic *scattering length*, with a material having a *scattering length density* (SLD)

$$(1) \rho = (1 - n^2) Q / 8\pi.$$

where Q is the reciprocal space scattering vector. Further, the scattering length density can be thought of as being comprised of nuclear and magnetic components

$$(2) \rho = \rho_{nuc} + \rho_{mag}.$$

The nuclear component of the scattering length density is defined as

$$(3) \rho_{nuc} = \sum_i b_i N,$$

where b is the characteristic nuclear scattering length of a given isotope, N is the number density, and the summation is over each isotope in the compound. Since the nuclear scattering lengths of the isotopes are known quantities (see <http://www.ncnr.nist.gov/resources/n-lengths/>), the nuclear scattering length density is directly related to the structural composition of a material. The magnetic component of the scattering length density is directly proportional to the sample magnetization M

$$(4) \rho_{mag} = (2.853 \times 10^{-9}) M,$$

for ρ in units of \AA^{-2} , and M in units of kA m^{-1} ($1 \text{ kA m}^{-1} = 1 \text{ emu cm}^{-3}$, for those of you not burdened by a need to use obscure SI units for magnetism).

Because each neutron is effectively a magnet with quantized spin, we can further enhance our sensitivity to a sample's magnetic structure by selecting only one of the neutron spin states in the incident and scattered beam. The utility of spin polarized neutrons is that they allow us to easily distinguish between the nuclear and magnetic components of the scattering length density. Using the formalism that + corresponds to neutron spin parallel to a magnetic field H , and - corresponds to neutron spin anti-parallel to H , we are interested in four polarized neu-

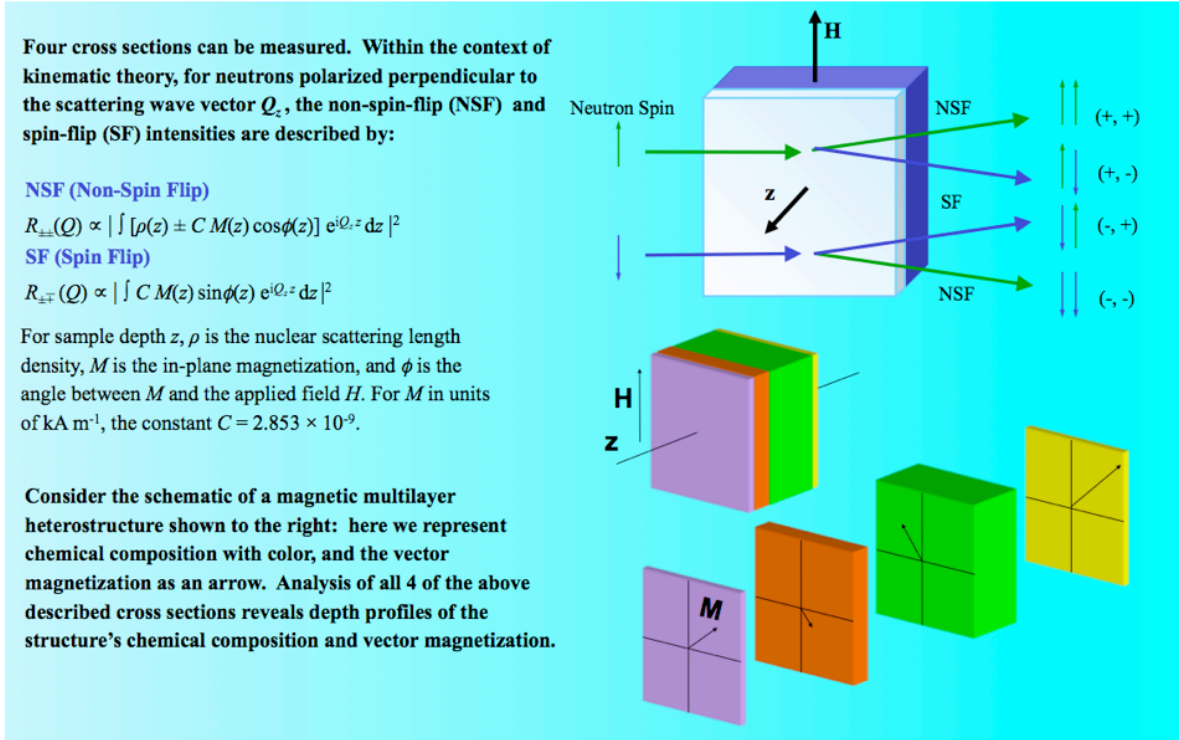


Figure 3: *Cartoon illustrating polarized neutron reflectometry.*

tron cross sections. The non spin-flip (incident and scattered neutrons have the same polarization) cross sections R^{--} and R^{++} are dependent on the nuclear depth profile, and the depth profile of the component of $M(z)$ parallel to H . The spin-flip cross sections R^{-+} and R^{+-} are purely magnetic in origin, and are dependent on the depth profile of the component of $M(z)$ perpendicular to H . A schematic of the PNR geometry is shown in Figure 3.

Oscillations in reflectometry spectra originate from interfaces between regions of differing scattering length density, with the amplitude of the oscillations depending on the magnitude of the contrast. The thickness of a given layer t is manifested in the period of an oscillation in Q -space (ΔQ). This can be qualitatively approximated as

$$(5) \quad t \approx 2\pi / \Delta Q .$$

For polarized neutrons, the in-plane component of the magnetization parallel to the neutron spin is manifest in different non spin-flip reflectivities for spin-up (R^{++}) and spin-down (R^{--}) neutrons, which are also sensitive to the nuclear scattering density. The in-plane component of the magnetization perpendicular to the neutron spin results in spin-flip scattering (R^{+-} , R^{-+}).

Quantitative information about a sample's real-space depth profile is determined by model fitting PNR spectra to a scattering length density profile.

Apparatus

For our measurement, we will use the NG-1 Polarized Beam Reflectometer. Figure 4 shows the beamline. A pyrolytic graphite [002] triple crystal monochromator intercepts a polychromatic cold neutron beam, and reflects a monochromatic beam (wavelength $\lambda = 4.75 \text{ \AA}$) down the beamline. Moving downstream, an Fe/Si supermirror is used to spin polarize the neutron beam. The magnetic field of the supermirror aligns the neutrons' spin along an axis normal to the floor, and its special layer structure causes one spin state (spin-up) to be reflected out of the beamline, while the other spin state (spin-down) is transmitted towards the sample. After the supermirror is a "Mezei" spin flipper, which consists of windings of aluminum (essentially transparent to neutrons) wire. When electrical current flows through the wires, the a magnetic field is produced that flips the neutron spin by

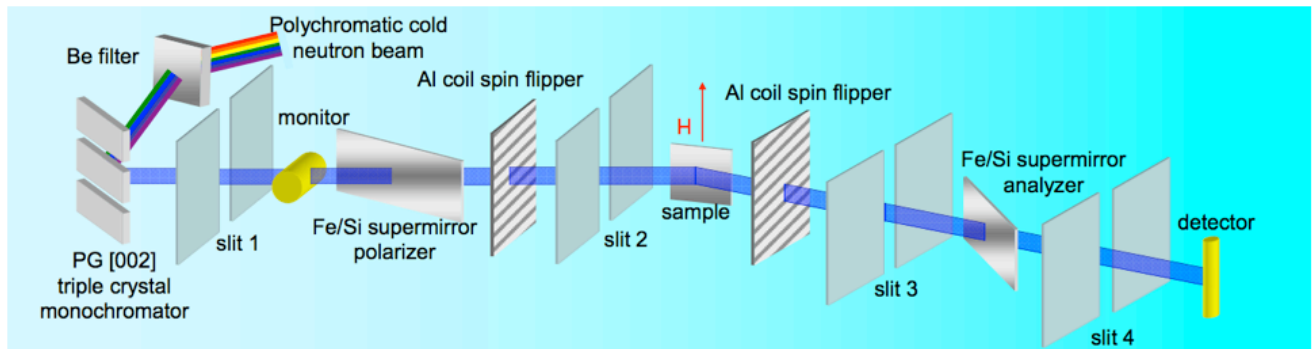


Figure 4: *Elements of the NG1 Polarized Neutron Reflectometer.*

180°, thus allowing the user the choice of spin-up or spin-down neutrons. The sample is inside the aluminum tailpiece of “displex” refrigerator mounted in an electromagnet, which is attached to a rotatable sample table. On the downstream side of the sample is the detector arm, which houses another Mezei flipper / supermirror analyzer assembly followed by a narrow “pencil” neutron detector. Like the polarizer, the analyzer supermirror transmits only spin-down neutrons, thus the downstream assembly allows for measurement of all four polarization cross-sections (- -, +-, -+, and ++). Since this instrument utilizes highly collimated incident and scattered beams, achieving a high degree of neutron polarization is not difficult. Typically, the beam polarization is greater than 95 %, and polarization corrections to the data are minor.

Experiment

Our sample is a 15x12 mm sample of the $x = 0.47$ LMO/LSO superlattice on a 1 mm thick SrTiO₃ substrate as described in the introduction. Confirmed by x-ray reflectometry, the structure is

{[0.40 nm LMO / 0.37 nm SMO] x5 / 0.40 nm LMO / [0.40 nm LMO / 0.37 nm SMO] x4}x4 / SrTiO₃ substrate

as shown in the Figure 2 cartoon. For our experiment we will use PNR to measure the *magnetic* depth profile of the sample at 120 K in 800 mT G. For our purposes we will assume that the structural composition determined from x-ray reflectometry measurements (not shown) are correct. Additionally, we know the nuclear scattering length densities for each of the component layers are (units of 10⁻⁶ Å⁻²)

$$\text{LMO: } \rho_{nuc} = 3.64, \text{ SMO: } \rho_{nuc} = 3.65, \text{ SrTiO}_3: \rho_{nuc} = 3.53.$$

Thus there is only about 0.1 % nuclear contrast between the LMO and SMO, and less than 2% contrast between the multilayer film and the substrate. Since it is the contrast between layers that gives rise to oscillations in the reflectivity, this means that our measurements won't be very sensitive to the *structural* profile of the multilayer film. Further, let's assume that in this large magnetic field, there is no

component of the *average* in-plane magnetization that is normal to the field direction, and therefore spin-flip scattering can be neglected. With this knowledge in hand, we can calculate PNR spectra for the sample, corresponding to different magnetic models prior to performing the experiment.

MODEL 1) ZERO MAGNETIZATION

What if our multilayer is totally nonmagnetic? In this case we have zero net magnetization, and thus, zero magnetic scattering length density. The profiles and corresponding PNR calculation for this case are shown in Figure 5. With no magneti-

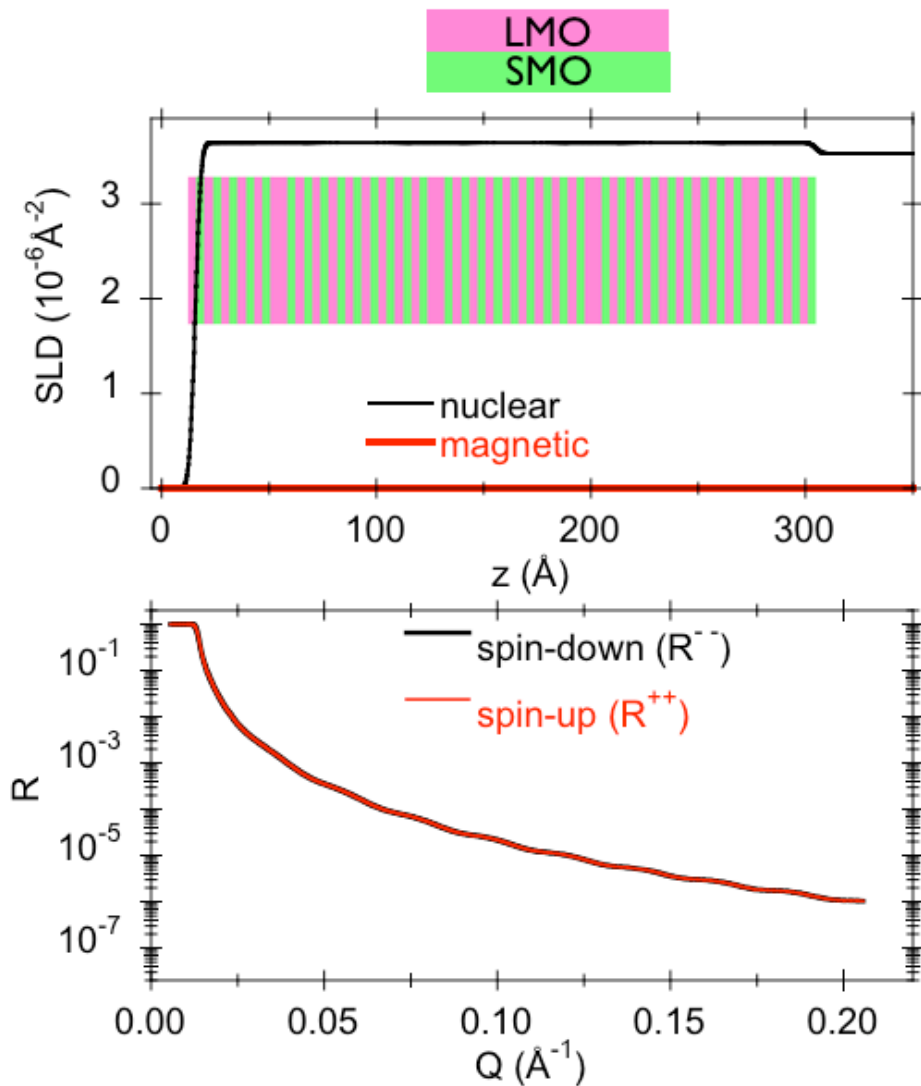


Figure 5: Nuclear and magnetic depth profiles (top) and calculated reflectivities corresponding to zero magnetization in the LMO/SMO multilayer stack

zation, the spin-up and spin-down reflectivities (R^{++} and R^{--}) are identical, each exhibiting very weak oscillations corresponding to the very weak nuclear contrast between the superlattice stack and the SrTiO₃ substrate.

MODEL 2) UNIFORM MAGNETIZATION

What if the multilayer has a totally uniform magnetization (as might be expected if the range of influence of the symmetry breaking is large)? For bulk LSMO, the saturation magnetic moment is approximately $m = (4-x) \mu_B / \text{Mn}$. If we assume that magnetic moment, we can convert to magnetic scattering length density via

$$(2) \rho_{mag} = 2.645 \times 10^{-5} \text{ N m},$$

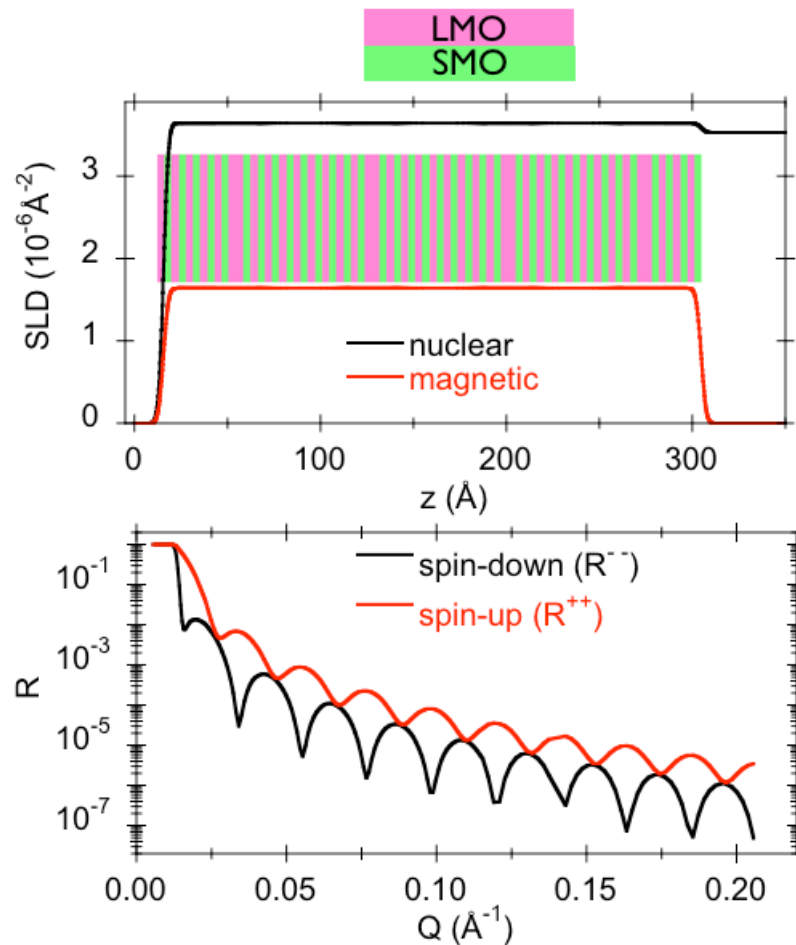


Figure 6: Nuclear and magnetic depth profiles (top) and calculated reflectivities corresponding to a uniform $(4-x) \mu_B / \text{Mn}$ magnetic moment

Where $N \approx 0.0176 \text{ \AA}^{-3}$ for our sample. The profiles and PNR calculations for this case are shown in Figure 6. We see that the spin-up and spin-down reflectivities are quite different, each exhibiting a Q -dependent “ringing” that is out of phase with the other.

MODEL 3) MODULATED MAGNETIZATION

What if the extra LMO layer influences it’s neighboring layers in a spatially dependent way (corresponding to a small range of influence)? For example, consider the case where the doubly thick LMO layer, and the unit cells of SMO on either side exhibit the saturation $m = (4-x) \mu_B / \text{Mn}$, and all other layers have zero

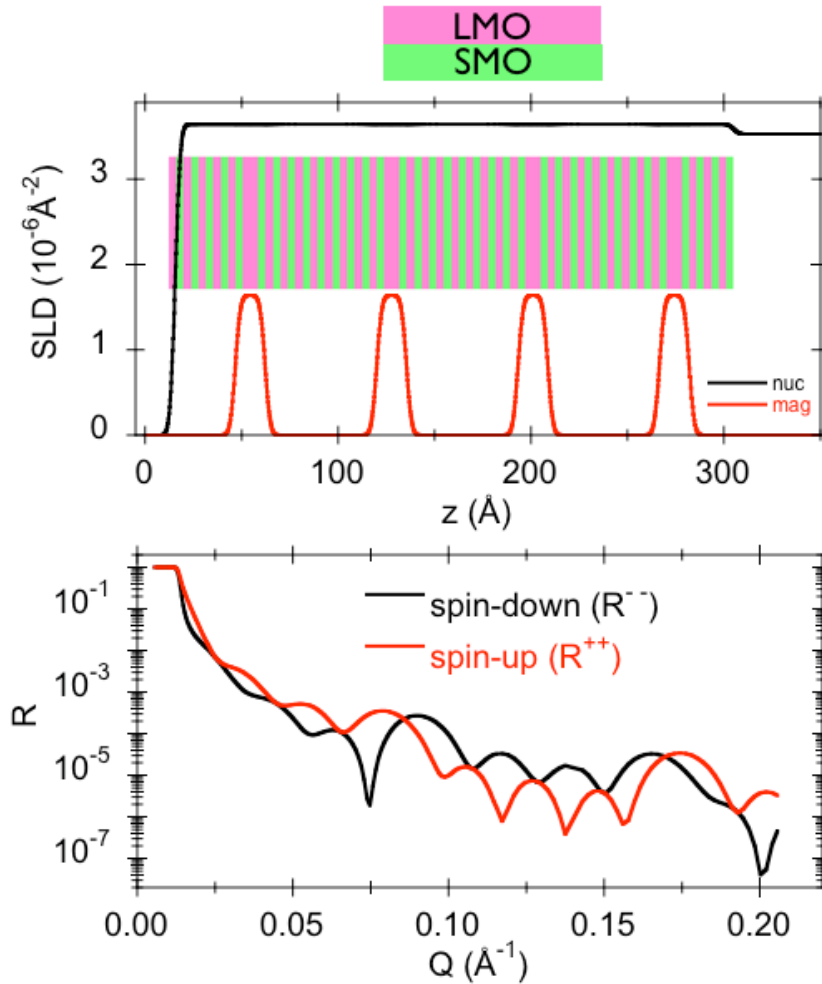


Figure 7: Nuclear and magnetic depth profiles (top) and calculated reflectivities corresponding to a modulated magnetic profile. The “thick” LMO layers and the SMO unit cells immediately surrounding them are magnetized at $(4-x) \mu_B / \text{Mn}$, all other layers have zero moment

magnetization. This case constitutes a real-space periodic magnetic structure of $T = 15 \text{ \AA}$ magnetized + 58 \AA unmagnetized = 73 \AA as shown in Figure 7. Thus, we can expect enhanced Bragg scattering at $Q = 2n\pi / T$, where $n = 1, 2, 3 \dots$. Such enhanced scattering is evident in the calculated scattering, near $Q = 0.08 \text{ \AA}^{-1}$, and $Q = 0.17 \text{ \AA}^{-1}$.

After conducting our PNR measurement, we will compare the measured scattering to the three basic models discussed above. Using the constraints of the model that best approximates the data, we will then optimize the real space parameters of interest (layer thickness, layer magnetization, etc.) to exactly fit the data, and thereby determine the magnetic depth profile. The goal will be to determine if the magnetization is modulated, and if so, to then determine the range of influence of the “extra” LMO layer via the periodicity of the modulation.

[1] J. F. Mitchell *et al.*, *J. Phys. Chem. B*, **105**, 10735 (2001).

[2] P.-G. de Gennes, *Phys. Rev.* **118**, 141 (1960).

[3] J. Hemberger, *et al.*, *Phys. Rev. B*, **66**, 094410 (2002).

[4] T. Santos, *et al.*, *Phys. Rev. B* **80**, 155114 (2009).